The Journal of Immunology

RESEARCH ARTICLE | JULY 01 2010

NADPH Oxidase-Dependent Reactive Oxygen Species Mediate Amplified TLR4 Signaling and Sepsis-Induced Mortality in Nrf2-Deficient Mice FREE

Xiaoni Kong; ... et. al

J Immunol (2010) 185 (1): 569–577.
https://doi.org/10.4049/jimmunol.0902315

NADPH Oxidase-Dependent Reactive Oxygen Species Mediate Amplified TLR4 Signaling and Sepsis-Induced Mortality in Nrf2-Deficient Mice

Xiaoni Kong,*[,1] Rajesh Thimmulappa,*[,1] Ponvijay Kombairaju,* and Shyam Biswal*[,†]

Sepsis syndrome is characterized by a dysregulated inflammatory response to infection. NADPH oxidase-dependent reactive oxygen species (ROS) play significant roles in the pathophysiology of sepsis. We previously showed that disruption of Nrf2, a master regulator of antioxidant defenses, caused a dysregulation of innate immune response that resulted in greater mortality in a polymicrobial sepsis and LPS shock model; however, the underlying mechanisms are unclear. In the current study, compared with wild-type ($Nrf2^{+/+}$) macrophages, we observed greater protein kinase C-induced NADPH oxidase-dependent ROS generation in Nrf2-disrupted ($Nrf2^{-/-}$) macrophages that was modulated by glutathione levels. To address the NADPH oxidase-mediated hyperinflammatory response and sepsis-induced lung injury and mortality in $Nrf2^{-/-}$ mice, we used double knockout mice lacking Nrf2 and NADPH oxidase subunit, $gp91^{phox}$ ($Nrf2^{-/-}$//$gp91^{phox-/-}$). Compared with $Nrf2^{+/+}$ macrophages, LPS induced greater activation of TLR4 as evident by TLR4 surface trafficking and downstream recruitment of MyD88 and Toll/IL-1R domain-containing adaptor in $Nrf2^{-/-}$ macrophages that was diminished by ablation of $gp91^{phox}$. Similarly, phosphorylation of IκB and IFN regulatory factor 3 as well as cytokine expression was markedly higher in $Nrf2^{-/-}$ macrophages; whereas, it was similar in $Nrf2^{+/+}$ and $Nrf2^{-/-}$//$gp91^{phox-/-}$. In vivo studies showed greater LPS-induced pulmonary inflammation in $Nrf2^{-/-}$ mice that was significantly reduced by ablation of $gp91^{phox}$. Furthermore, LPS shock and polymicrobial sepsis induced early and greater mortality in $Nrf2^{-/-}$ mice; whereas, $Nrf2^{-/-}$//$gp91^{phox-/-}$ showed prolong survival. Together, these results demonstrate that Nrf2 is essential for the regulation of NADPH oxidase-dependent ROS-mediated TLR4 activation and lethal innate immune response in sepsis. ***The Journal of Immunology*****, 2010, 185: 569–577.**

Despite advances in antibiotic treatment and critical care, sepsis remains a major cause of mortality in intensive care units. Sepsis is characterized by an overwhelming systemic inflammatory response to bacterial infection (1). TLR4 recognizes Gram negative bacteria and bacterial components (LPS) and thereby mediates innate immune cell activation (2, 3). On LPS binding, TLR4 undergoes homodimerization and through the cytoplasmic Toll/IL-1R homology domain, recruits the adapter molecule myeloid differentiation marker 88 (MyD88) and/or Toll/IL-1R homology domain-containing adaptor (TRIF) to initiate signal transduction (2, 3). Recent studies have shown that reactive oxygen species (ROS) play crucial roles in TLR4 activation and the pathobiology of sepsis by regulating immune cell activation and end-organ injury (4). Excess intracellular and extracellular ROS (superoxide, hydrogen peroxide) have the ability to prime the phagocytes (macrophages and neutrophils) against an acute hyperinflammatory response (5–7). Host factors that regulate cellular ROS levels may act as important modifiers in pathogenesis of sepsis (8).

The NADPH oxidase complex is a major source of intracellular ROS generation in macrophages and neutrophils (9). The NADPH oxidase complex is composed of two transmembrane proteins: flavocytochrome b components ($gp91^{phox}$ and $p22^{phox}$) and four cytosolic proteins ($p47^{phox}$, $p67^{phox}$, $p40^{phox}$, and Rac) (9). On activation, the cytosolic components translocate to the transmembrane catalytic protein $gp91^{phox}$, which results in the formation of functional NADPH oxidase complex. ROS has been implicated in multiple physiological and pathological processes as a secondary messenger in cell signaling (10). Numerous studies have demonstrated the role of NADPH oxidase-dependent ROS generation in modulating TLR4 signaling, inflammatory response (11), and disease pathogenesis (7, 12).

Nrf2, a bZIP transcription factor, plays an essential role in the regulation of redox homeostasis and cytoprotective defenses (13). In response to oxidative stress, Nrf2 dissociates from its cytoplasmic inhibitor Keap1 and regulates genes containing a *cis*-acting element termed antioxidant response element that includes genes encoding for antioxidant defenses, NADPH-regenerating enzymes, and xenobiotic detoxification enzymes. Nrf2-regulated antioxidant-associated defenses comprise glutathione (GSH) biosynthesizing enzymes, glutamate-cysteine ligase modifier subunit (Gclm) and catalytic subunit, glutathione reductase, glutathione

*Department of Environmental Health Sciences, Bloomberg School of Public Health and †Division of Pulmonary and Critical Care Medicine, School of Medicine, The Johns Hopkins University, Baltimore, MD 21205

[1]X.K. and R.T. contributed equally to this work.

Received for publication July 17, 2009. Accepted for publication April 10, 2010.

This work was supported by National Institutes of Health Grants GM079239 (to S.B.) and HL081205 (to S.B.), National Heart, Lung, and Blood Institute Specialized Centers of Clinically Oriented Research Grant P50HL084945 (to S.B.), Center for Childhood Asthma in the Urban Environment Grant P50ES015903, National Institute on Environmental Health Sciences Center Grant P30 ES003819, a Clinical Innovator Award from Flight Attendant Medical Research Institute (to S.B.), and Young Clinical Scientist Awards from Flight Attendant Medical Research Institute (to R.K.T.).

Address correspondence and reprint requests to Dr. Shyam Biswal, Department of Environmental Health Sciences, Bloomberg School of Public Health, The Johns Hopkins University, 615 North Wolfe Street, Baltimore, MD 21205. E-mail address: sbiswal@jhsph.edu

The online version of this article contains supplemental material.

Abbreviations used in this paper: AU, arbitrary unit; BAL, bronchoalveolar lavage; BSO, buthionine-sulfoximine; CLP, cecal ligation and puncture; Gclm, glutamate-cysteine ligase modifier subunit; GSH, glutathione; IRF, IFN regulatory factor; MCF, mean channel fluorescence; Nqo1, NAD(P)H quinone oxidoreductase 1; PKC, protein kinase C; QRT-PCR, quantiative real-time PCR; RFC, relative fold change; ROS, reactive oxygen species; TRIF, Toll/IL-1R homology domain-containing adaptor.

peroxidase 2, catalase, NADPH-synthesizing enzyme glucose-6-phosphate dehydrogenase, NAD(P)H quinone oxidoreductase 1 (Nqo1), heme oxygenase 1, and thioredoxin reductase 1 (13). Disruption or defective activity of Nrf2 sensitizes cells to detrimental effects of environmental toxicants and predisposes mice to several oxidative and inflammatory disorders that include emphysema, asthma, acute lung injury, fibrosis, neurodegenerative diseases, stroke, liver cirrhosis, colitis, and age-related autoimmune diseases (13–21). The pathogenesis of these disorders in Nrf2-deficient ($Nrf2^{-/-}$) mice is mediated largely by oxidative stress.

Recently, we and others have reported that, in addition to the heightened sensitivity to chemical toxicants, $Nrf2^{-/-}$ mice are also more sensitive to bacteria and LPS-mediated inflammation (17, 22, 23). In a model of acute peritonitis and LPS-induced shock, $Nrf2^{-/-}$ mice showed early and greater mortality compared with $Nrf2^{+/+}$ mice. Similarly, LPS challenge induced hyperinflammation in the lungs of $Nrf2^{-/-}$ mice. Global gene expression analysis by microarray revealed markedly augmented expression of cytokines, chemokines, adhesion molecules, and other effectors of innate immune response in the lungs of $Nrf2^{-/-}$ mice compared with the lungs of $Nrf2^{+/+}$ mice after a sublethal LPS challenge (17). LPS stimulation resulted in greater IKK kinase activity and subsequent phosphorylation of IκB and nuclear translocation of NF-κB in $Nrf2^{-/-}$ macrophages compared with $Nrf2^{+/+}$ macrophages. However, upstream signaling events responsible for amplified innate immune response in $Nrf2^{-/-}$ are unknown. Although $Nrf2^{-/-}$ macrophages displayed greater LPS-induced ROS levels compared with $Nrf2^{+/+}$ macrophages (17, 24), it is unclear whether or how ROS mediate dysregulation of the inflammatory response and mortality in $Nrf2^{-/-}$ mice in response to LPS. We hypothesize that enhanced NADPH oxidase-dependent ROS mediate an overzealous inflammatory response by TLR4 activation and sepsis-induced mortality in $Nrf2^{-/-}$ mice. To address our hypothesis, we examined LPS-induced TLR4 activation and downstream signaling events in macrophages, lung inflammation, systemic inflammation, and mortality using $Nrf2^{+/+}$, $Nrf2^{-/-}$, $gp91^{phox-/-}$, and $Nrf2^{-/-}$//$gp91^{phox-/-}$ mice.

Materials and Methods

Mice

$Gp91^{phox}$-deficient ($gp91^{phox-/-}$) mice were obtained from The Jackson Laboratory (Bar Harbor, ME) and were crossed with $Nrf2^{-/-}$ C57BL/6J mice (25) to generate $Nrf2^{-/-}$//$gp91^{phox-/-}$ mice. Mice were housed in controlled conditions for temperature and humidity, using a 12 h light/dark cycle. All experimental protocols were performed in accordance with the standards established by the U.S. Animal Welfare Acts, as set forth in the National Institutes of Health (Bethesda, MD) guidelines and in the Policy and Procedures Manual of The Johns Hopkins University Animal Care and Use Committee.

LPS treatment

Mice were injected with either a sublethal (15 mg/kg body weight, i.p.; or 10 μg/mouse, intratracheal instillation) or a lethal dose of LPS (35 mg/kg body weight, i.p.) (*Escherichia coli*, serotype 055:B5; Sigma-Aldrich, St. Louis, MO). Lung inflammation was measured at 1 h or 6 h after LPS treatment. Mortality was monitored for 5 d.

Cecal ligation and puncture

Sepsis was induced by cecal ligation and puncture (CLP) using methods described previously (17). Briefly, a midline laparotomy was performed on the anesthetized mice, and the cecum was identified. The distal 50% of exposed cecum was ligated with 3-0 silk suture and punctured with one pass of a 20-gauge needle. The cecum was replaced in the abdomen, and the incision was closed with 3-0 suture. The animals were resuscitated after surgical operation using an s.c. injection of 1 ml sterile saline (0.9% NaCl). Mice were monitored regularly, and survival was recorded over a period of 7 d.

Bronchoalveolar lavage and phenotyping

Mice were anesthetized with an overdose of sodium pentobarbital. The lungs were lavaged two times using 1 ml of sterile PBS to collect the bronchoalveolar lavage (BAL) fluid. Cells were counted by using a hemocytometer, and a differential cell count was performed on 300 cells using Wright-Giemsa stain (Baxter, Deerfield, IL). Cell-free lavage was used for the analysis of cytokines.

Quantitative real-time PCR

Total RNA was extracted from macrophages or lungs by using Trizol (Invitrogen, Carlsbad, CA) according to the manufacturer's instructions. Total RNA (1 μg) was used for cDNA synthesis. Quantitative real-time PCR (QRT-PCR) analyses were performed by using commercially available probes from Applied Biosystems. Assays were performed by using the ABI 7000 Taqman system (Applied Biosystems, Carlsbad, CA). GAPDH was used for normalization. The data analysis was performed as described previously (24).

Isolation of peritoneal macrophages, neutrophils, and treatment

Peritoneal macrophages and neutrophils were isolated from mice after i.p. injection of 2–3 ml 3% thioglycolate, as described (17, 24). Cells were then treated with LPS or vehicle for various periods, and ROS, protein kinase C (PKC) activity, and GSH levels were measured. For treatment with PKC inhibitor, macrophages were treated with staurosporine (50 nM) for 1 h, followed by LPS stimulation.

Flow cytometry

Cell surface expression of TLR4 was detected by flow cytometry of live cells stained with FITC-conjugated anti-TLR4 Ab. A total of 10,000 cells per condition were analyzed using a FACScan (Becton Dickinson, San Jose, CA) with FL1 525 mM Band Pass detector at an excitation wavelength of 488 nm.

Measurement of ROS

Intracellular and mitochondrial levels of ROS were determined using the redox sensitive dyes carboxy-2',7'-dichlorodihydrofluorescein diacetate and MitoSOX (Molecular Probes, Eugene, OR), respectively, in conjunction with flow cytometry (26, 27).

Measurement of PKC activity

Macrophages were washed once with cold PBS and lysed in cell lysis buffer (Cell Signaling Technology, Danvers, MA). PKC activity was measured in whole cell lysates using Cyclex protein kinase C assay kit (CycLex, Nagano, Japan). Aliquots of lysates were used for protein estimation.

Measurement of GSH

Intracellular GSH was measured by luminometer using Promega GSH-Glo-glutathione Assay kit (Promega, Madison, WI).

Immunoblotting and immunoprecipitation

Immunoprecipitation and immunobloting were performed as described previously (17). Cell lysates and immunoprecipitated products were resolved on 8–16% $NaDodSO_4$ PAGE (SDS-PAGE), and the proteins were visualized by immunoblotting using Abs directed against the indicated Ags. Anti-TLR4, anti-MyD88, anti-IκB, and antiphosphorylated IκB Abs were obtained from Santa Cruz Biotechnology (Santa Cruz, CA). Anti-IFN regulatory factor (IRF)3 and antiphosphorylated IRF3 Abs were obtained from Cell Signaling Technology. Anti-TRIF was purchased from Abcam (Cambridge, MA).

Statistics

Student two-tailed t test was used to evaluate differences between the control and treatment groups within a single genotype as well as between genotypes. Survival studies were analyzed by using the log-rank test. Statistical significance was accepted at $p < 0.05$.

Results

Nrf2 regulate LPS-induced NADPH oxidase-dependent ROS generation by modulating PKC activation

Previously, we have reported that $Nrf2^{-/-}$ macrophages show higher levels of ROS after LPS stimulation (24). However, it is

unclear whether the higher levels of ROS are due to an inadequate antioxidant-mediated detoxification or greater generation of ROS. GSH is the major ROS-scavenging system in cells (28). Several ROS detoxification enzymes, including peroxidases, peroxiredoxins, and thiol reductases use reduced GSH as the source of reducing equivalents. We found that GSH levels were significantly higher in macrophages isolated from $Nrf2^{+/+}$ compared with $Nrf2^{-/-}$ mice (Fig. 1*A*). To investigate whether the lower levels of ROS in $Nrf2^{+/+}$ macrophages compared with $Nrf2^{-/-}$ macrophages are due to better ROS scavenging ability, we treated macrophages from both genotypes with or without L-buthioninesulfoximine [BSO, inhibitor of glutathione synthesis (29)] and stimulated with LPS. BSO (200 μM) treatment significantly depleted GSH, and the levels were comparable in $Nrf2^{+/+}$ and $Nrf2^{-/-}$ macrophages 16 h after BSO treatment (Fig. 1*A*). LPS stimulation resulted in 2-fold higher ROS levels in $Nrf2^{-/-}$ macrophages compared with $Nrf2^{+/+}$ macrophages (Fig. 1*B*). BSO pretreatment showed no further elevation of ROS levels in $Nrf2^{-/-}$ macrophages after LPS treatment. However, BSO pretreatment significantly augmented LPS-induced ROS levels in $Nrf2^{+/+}$ macrophages and the levels were comparable to that in LPS-stimulated $Nrf2^{-/-}$ macrophages (Fig. 1*B*). These data indicate that greater levels of GSH in $Nrf2^{+/+}$ may be partly responsible for diminished ROS levels after LPS stimulation.

Next, we investigated whether generation of ROS is greater in $Nrf2^{-/-}$ macrophages compared with $Nrf2^{+/+}$ macrophages. As NADPH oxidase is the primary generator of ROS after LPS stimulation, we chose to assess the activation of NADPH oxidase by measuring phosphorylation of $p47^{phox}$. Phosphorylation of $p47^{phox}$ is a critical step for the assembly of the NADPH oxidase complex (9). As shown in Fig. 1*C* and 1*D*, $Nrf2^{-/-}$ macrophages showed greater phosphorylation of $p47^{phox}$ compared with $Nrf2^{+/+}$ macrophages after stimulation with LPS. Phosphorylation of $p47^{phox}$ is mediated by PKC after LPS stimulation in neutrophils and macrophages (30, 31). Therefore, we next analyzed total PKC activity in $Nrf2^{+/+}$ and $Nrf2^{-/-}$ macrophages 30 min after LPS stimulation. Vehicle-treated $Nrf2^{+/+}$ and $Nrf2^{-/-}$ macrophages showed similar PKC activity (Fig. 1*E*). However, LPS treatment resulted in significantly greater PKC activity in $Nrf2^{-/-}$ macrophages compared with $Nrf2^{+/+}$ macrophages (Fig. 1*E*). Cellular GSH has been shown to inhibit PKC activation (32, 33). To determine whether higher GSH levels in $Nrf2^{+/+}$ macrophages attenuated PKC activation, we measured PKC activity after GSH depletion by BSO treatment. BSO pretreatment elevated LPS- induced PKC activity in $Nrf2^{+/+}$ macrophages, and the PKC activity was comparable to that of LPS-treated $Nrf2^{-/-}$ macrophages (Fig. 1*E*). We did not observe any significant changes in PKC activity in LPS-treated $Nrf2^{-/-}$ macrophages with or without BSO pretreatment. Finally, to determine whether PKC activity was responsible for higher ROS generation in $Nrf2^{-/-}$ macrophages, we measured ROS levels after LPS stimulation in the presence of the PKC inhibitor, staurosporine (STS) (34). STS significantly attenuated LPS-induced ROS generation in $Nrf2^{-/-}$ and $Nrf2^{+/+}$ macrophages (Fig. 1*F*). Overall, these results indicate that Nrf2-dependent regulation of GSH modulates NADPH oxidase activity by suppressing PKC activity.

Disruption of NADPH oxidase suppresses LPS-induced ROS generation in $Nrf2^{-/-}$ macrophages

To further demonstrate that NADPH oxidase activity is the major source of ROS in $Nrf2^{-/-}$ cells, we generated double knockout mice that lack the NADPH oxidase transmembrane component, $gp91^{phox}$ and Nrf2 by crossing $Nrf2^{-/-}$ and $gp91^{phox-/-}$ mice. The double knockout mice ($Nrf2^{-/-}$//$gp91^{phox-/-}$) were fertile and showed no abnormal phenotype. The genotyping results are described in Supplemental Fig. 1. In response to LPS stimulation, ROS

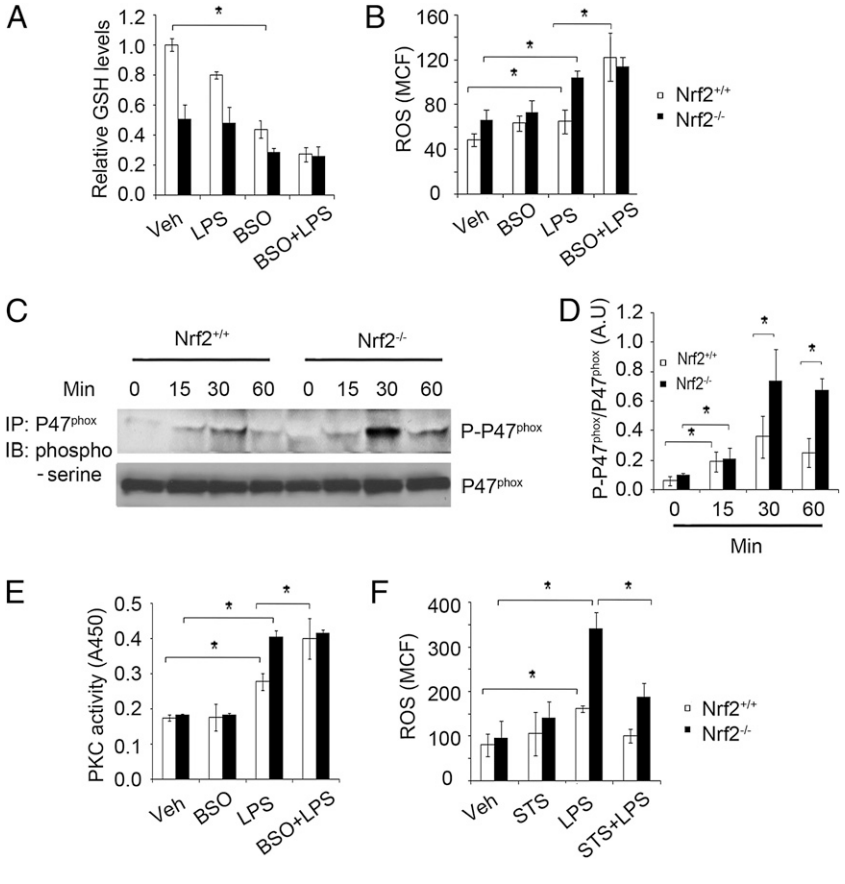

FIGURE 1. LPS induced greater activation of NADPH oxidase in $Nrf2^{-/-}$ macrophages by modulating PKC. *A* and *B*, Intracellular levels of GSH (*A*) and ROS (*B*) in $Nrf2^{-/-}$ and $Nrf2^{+/+}$ macrophages treated with or without BSO (200 μM) for 16 h, followed by LPS stimulation (1 h). *C*, Levels of phosphorylated-serine and $p47^{phox}$ in $Nrf2^{-/-}$ and $Nrf2^{+/+}$ macrophages after LPS stimulation. After LPS activation, cell lysates were prepared and immunoprecipatated using anti-$p47^{phox}$ Abs. The immune complex was resolved on SDS-PAGE and levels of phosphorylated-serine and $p47^{phox}$ were analyzed using antiphosphorylated serine and anti-$p47^{phox}$ Abs by Western blot analysis. *D*, Densitometry analysis of phosphorylated-$p47^{phox}$ immunoblot normalized to total $p47^{phox}$ using ImageJ software. Data are represented as mean ± SD, AUs from three independent experiments. *E*, PKC activity in $Nrf2^{-/-}$ and $Nrf2^{+/+}$ macrophages treated with or without BSO for 16 h, followed by LPS stimulation (30 min). *F*, Flow cytometric analysis of ROS in $Nrf2^{-/-}$ and $Nrf2^{+/+}$ macrophages treated with or without STS for 30 min, followed by LPS stimulation (1 h). Analysis of ROS was performed within 3 h after macrophage isolation. Data are represented MCF from two independent experiments ($n = 3$). $*p < 0.05$. AU, arbitrary unit; MCF, mean channel fluorescence.

generation was significantly diminished in Nrf2$^{-/-}$//gp91$^{phox-/-}$ compared with Nrf2$^{-/-}$ macrophages (Fig. 2*A*). Similar results were observed in neutrophils derived from Nrf2$^{-/-}$// gp91$^{phox-/-}$ and Nrf2$^{-/-}$ mice (Fig. 2*B*). As expected, among the genotypes, ROS level was lowest in macrophages and neutrophils from gp91$^{phox-/-}$ mice after LPS stimulation. Of considerable interest, we noted moderate but significantly higher levels of ROS in macrophages from Nrf2$^{-/-}$//gp91$^{phox-/-}$ mice compared with gp91$^{phox-/-}$ mice suggesting ROS generation by an NADPH oxidase independent mechanism. In addition to NADPH oxidase, the other major source of cellular ROS is mitochondrial activity after LPS stimulation (35, 36). To monitor the mitochondrial origin of ROS after LPS stimulation, we used fluoroprobe MitoSOX Red that enters viable cells and specifically targets mitochondria. Flow cytometric analysis revealed relatively greater mitochondrial ROS levels in macrophages from Nrf2$^{-/-}$ mice compared with Nrf2$^{+/+}$ macrophages after LPS stimulation (Fig. 2*C*). However, we found similar levels of mitochondrial ROS in macrophages from Nrf2$^{-/-}$ and Nrf2$^{-/-}$//gp91$^{phox-/-}$ mice after LPS treatment (Fig. 2*C*). The expression of Nrf2-regulated genes (Nqo1, Gclm) was similar in Nrf2$^{-/-}$//gp91$^{phox-/-}$ and Nrf2$^{-/-}$ macrophages and was significantly higher in Nrf2$^{+/+}$ macrophages (Fig. 2*D*). Taken together, these results demonstrate that NADPH oxidase is the primary source; whereas, mitochondria is the secondary source of ROS production that contributes to elevated ROS levels in Nrf2$^{-/-}$ macrophages after LPS stimulation.

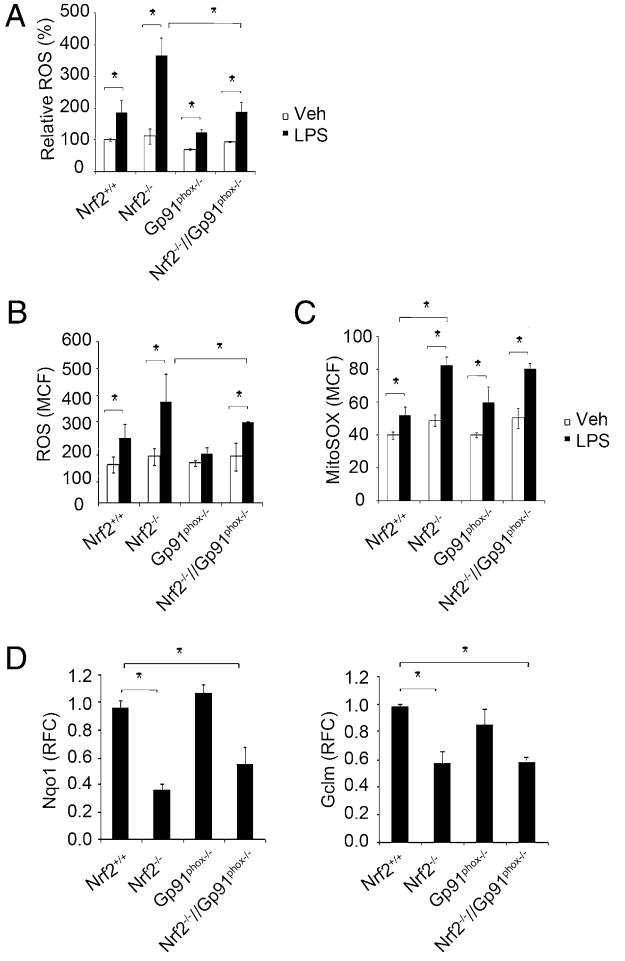

FIGURE 2. Disruption of NADPH oxidase reduces LPS-induced ROS generation in Nrf2$^{-/-}$ macrophages. *A* and *B*, Flow cytometric analysis of ROS in Nrf2$^{+/+}$, Nrf2$^{-/-}$, gp91$^{phox-/-}$, and Nrf2$^{-/-}$//gp91$^{phox-/-}$ macrophages (*A*) and neutrophils (*B*) after LPS treatment (1 h). Data are represented as mean percentage change compared with vehicle-treated Nrf2$^{+/+}$ from three independent experiments. *C*, Flow cytometric analysis of mitochondrial ROS levels in macrophages from Nrf2$^{+/+}$, Nrf2$^{-/-}$, gp91$^{phox-/-}$, and Nrf2$^{-/-}$//gp91$^{phox-/-}$ mice after LPS treatment. Data are represented as MCF ± SD from three independent experiments. *D*, mRNA expression of Gclm and Nqo1 genes in unstimulated peritoneal macrophages from Nrf2$^{+/+}$, Nrf2$^{-/-}$, gp91$^{phox-/-}$, and Nrf2$^{-/-}$//gp91$^{phox-/-}$ mice by QRT-PCR. $*p < 0.05$. MCF, mean channel fluorescence

Disruption of gp91^{phox} in Nrf2$^{-/-}$ macrophages alleviate TLR4 surface trafficking in response to LPS

In the case of Gram-negative bacterial infection, activation of TLR4 signaling is the earliest event in the pathogenesis of sepsis (37, 38). Recent studies have reported that ROS modulate TLR4 signaling partly by enhancing surface trafficking of TLR4 from the cytoplasm (39, 40). To decipher whether Nrf2-dependent ROS generation modulates TLR4 surface trafficking, we investigated surface expression of TLR4 in macrophages isolated from Nrf2$^{+/+}$, Nrf2$^{-/-}$, gp91$^{phox-/-}$, and Nrf2$^{-/-}$//gp91$^{phox-/-}$ mice 1 h after LPS treatment by flow cytometry. LPS stimulation significantly enhanced surface trafficking of TLR4 in macrophages and neutrophils of all genotypes compared with vehicle treatment (Fig. 3*A*, 3*B*). Consistent with ROS levels, Nrf2$^{-/-}$ macrophages showed a higher level of TLR4 surface trafficking compared with Nrf2$^{+/+}$ macrophages after LPS treatment. On the contrary, ablation of gp91^{phox} in Nrf2$^{-/-}$ macrophages significantly decreased surface trafficking of TLR4 (Fig. 3*A*) after LPS stimulation. Similarly, a higher surface expression of TLR4 was observed in Nrf2$^{-/-}$ neutrophils compared with Nrf2$^{+/+}$ after LPS stimulation that was significantly reduced by disruption of the NADPH oxidase complex (Fig. 3*B*). In line with levels of ROS, the TLR4 surface expression between Nrf2$^{+/+}$ and Nrf2$^{-/-}$//gp91$^{phox-/-}$ macrophages was comparable after LPS stimulation. Among the

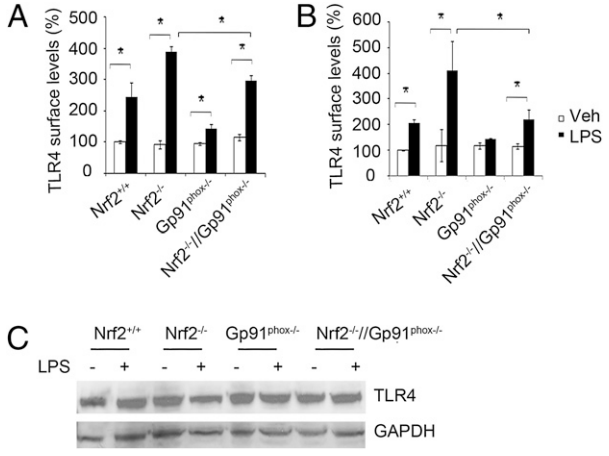

FIGURE 3. Ablation of gp91^{phox} reduced LPS-induced surface trafficking of TLR4 in macrophages from Nrf2$^{-/-}$ mice. *A*, Surface expression of TLR4 in macrophages of Nrf2$^{+/+}$, Nrf2$^{-/-}$, gp91$^{phox-/-}$, and Nrf2$^{-/-}$// gp91$^{phox-/-}$ mice 1 h after LPS treatment by FACS analysis as described in *Materials and Methods*. Data are presented as percentage compared with Nrf2$^{+/+}$ vehicle and are mean ± SD from three independent experiments ($n = 3$). *B*, Surface expression of TLR4 in neutrophils of Nrf2$^{+/+}$, Nrf2$^{-/-}$, gp91$^{phox-/-}$, and Nrf2$^{-/-}$//gp91$^{phox-/-}$ mice 1 h after LPS treatment by FACS analysis as described in *Materials and Methods*. Data are presented as percentage compared with Nrf2$^{+/+}$ vehicle and are mean ± SD from three independent experiments ($n = 3$). *C*, Total TLR4 protein in macrophages from Nrf2$^{+/+}$, Nrf2$^{-/-}$, and Nrf2$^{-/-}$//gp91$^{phox-/-}$ mice with or without LPS stimulation. After LPS activation, cell lysates were prepared and total TLR4 protein levels were measured by immunoblot analysis. GAPDH was used as a loading control. $*p < 0.05$.

genotypes, macrophages and neutrophils from gp91$^{phox-/-}$ mice showed the lowest TLR4 surface expression after LPS stimulation. We also investigated whether Nrf2 affects the levels of total TLR4 in cells. As shown in Fig. 3*C*, we found no significant difference in the basal levels of total endogenous TLR4 protein between Nrf2$^{-/-}$, Nrf2$^{+/+}$, gp91$^{phox-/-}$, and Nrf2$^{-/-}$//gp91$^{phox-/-}$ macrophages. These results suggest that enhanced NADPH oxidase-induced ROS is largely responsible for heightened TLR4 signaling in Nrf2$^{-/-}$ macrophages.

Disruption of gp91^{phox} in Nrf2$^{-/-}$ macrophages reduces recruitment of MyD88 and TRIF to TLR4 and subsequent activation of NF-κB and IRF3 after LPS stimulation

To determine whether higher surface trafficking of TLR4 leads to greater recruitment of downstream adapter molecules, we analyzed TLR4–MyD88 and TLR–TRIF complex formation in macrophages after LPS treatment. Cell lysates were subjected to immunoprecipitation using an anti-TLR4 Abs, and the immune complexes were analyzed by Western blot analysis using anti-MyD88 and anti-TRIF Abs. After LPS stimulation, the levels of MyD88 and TRIF interacting with TLR4 were elevated in macrophages from all genotypes (Fig. 4*A*, 4*B*). LPS stimulation led to greater recruitment of MyD88 and TRIF to TLR4 in Nrf2$^{-/-}$ macrophages compared with Nrf2$^{+/+}$ macrophages, which was consistent with the surface trafficking of TLR4. However, disruption of gp91^{phox} in Nrf2$^{-/-}$ macrophages significantly decreased levels of TLR4–MyD88 and TLR4–TRIF complexes and it was comparable to that in the LPS-treated Nrf2$^{+/+}$ macrophages (Fig. 4*A*, 4*B*). The MyD88-dependent pathway of TLR4 leads to activation of NF-κB; whereas, the TRIF-dependent pathway of TLR4 leads to activation of the IRF3 transcription factor (3). As markers of NF-κB and IRF3 activation, we analyzed phosphorylation of IκB and IRF3 in Nrf2$^{+/+}$, Nrf2$^{-/-}$, gp91$^{phox-/-}$, and Nrf2$^{-/-}$//gp91$^{phox-/-}$ macrophages after LPS challenge. Nrf2$^{-/-}$ macrophages showed higher levels of phosphorylation of IκB and IRF3 compared with Nrf2$^{+/+}$ macrophages (Fig. 4*C*, 4*D*). However, disruption of gp91^{phox} significantly decreased phosphorylation of IκB and IRF3 in Nrf2$^{-/-}$ macrophages. The levels of phosphorylated IκB and IRF3 were similar in LPS-treated Nrf2$^{+/+}$ and Nrf2$^{-/-}$//gp91$^{phox-/-}$ macrophages (Fig. 4*C*, 4*D*). In agreement with the TLR4 surface expression, the levels of TLR4–MyD88 and TLR4–TRIF complex as well as phosphorylation of IκB and IRF3 were lowest in LPS-treated macrophages isolated from gp91$^{phox-/-}$ mice.

Disruption of gp91^{phox} in Nrf2$^{-/-}$ macrophages reduced LPS-induced expression of cytokines

We next investigated whether upstream TLR4 signaling events corroborate with degree of cytokine expression in Nrf2$^{+/+}$, Nrf2$^{-/-}$, gp91$^{phox-/-}$, and Nrf2$^{-/-}$//gp91$^{phox-/-}$ macrophages after LPS treatment. Overall, gp91$^{phox-/-}$ macrophages showed a lower expression of cytokines (IL-6, MCP-1, MIP-2, IFN-β, IP-10, and RANTES) after LPS challenge (Fig. 5). In contrast to Nrf2$^{+/+}$ macrophages, Nrf2$^{-/-}$ macrophages showed greater expression of all cytokines after LPS stimulation. In contrast, the expression of these cytokines was significantly diminished in Nrf2$^{-/-}$//gp91$^{phox-/-}$ macrophages compared with Nrf2$^{-/-}$ macrophages. The levels of cytokines were similar in Nrf2$^{+/+}$ and Nrf2$^{-/-}$//gp91$^{phox-/-}$ macrophages after LPS challenge.

Disruption of gp91^{phox} in Nrf2$^{-/-}$ mice alleviates pulmonary inflammation after LPS treatment

We have reported that Nrf2$^{-/-}$ mice show greater pulmonary inflammation compared with Nrf2$^{+/+}$ mice after LPS treatment (17, 24). To determine whether elevated TLR4 activation by

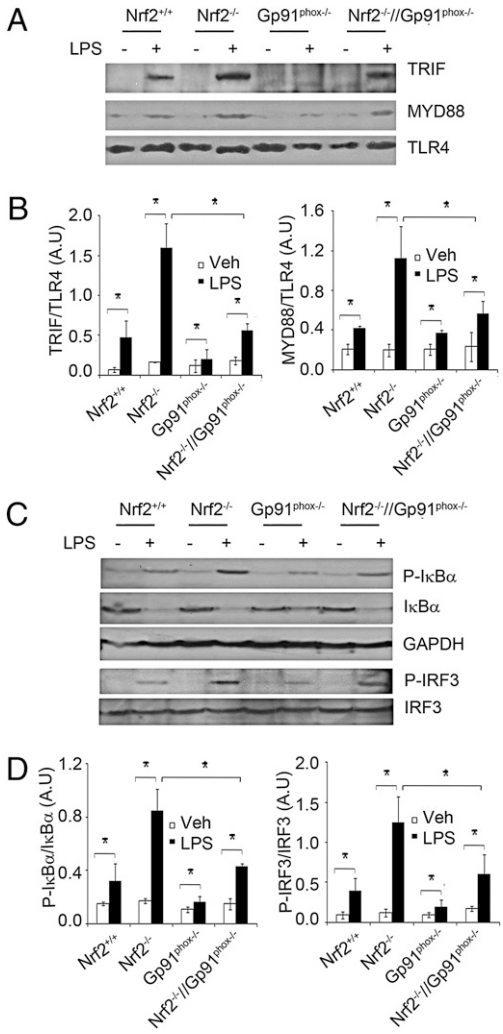

FIGURE 4. Genetic disruption of gp91^{phox} in Nrf2$^{-/-}$ macrophages decreases recruitment of MyD88 and TRIF to TLR4 and inhibits NF-κB and IRF3 activation after LPS stimulation. *A*, Levels of TLR4–MyD88 and TLR4–TRIF complex in macrophages from Nrf2$^{+/+}$, Nrf2$^{-/-}$ gp91$^{phox-/-}$, and Nrf2$^{-/-}$//gp91$^{phox-/-}$ mice after LPS stimulation. After LPS activation, cell lysates were prepared and immunoprecipitated using anti-TLR4 Abs. The immune complex was resolved on SDS-PAGE and the levels of MyD88, TRIF, and TLR4 were analyzed by Western blot analysis. *B*, Densitometry analysis of immunoblot normalized to GAPDH using ImageJ software. Data are represented as mean ± SD, AUs from three independent experiments. *C*, Levels of phosphorylated-IκB, phosphorylated-IRF3, total IκB, and IRF3 in macrophage from Nrf2$^{+/+}$, Nrf2$^{-/-}$, gp91$^{phox-/-}$, and Nrf2$^{-/-}$//gp91$^{phox-/-}$ mice after LPS stimulation as evaluated by Western blot analysis. *D*, Densitometry analysis of immunoblot normalized to GAPDH using ImageJ software. Data are represented as mean ± SD, AUs from three independent experiments. $*p < 0.05$. AU, arbitrary unit.

NADPH oxidase-dependent ROS generation is responsible for exaggerated inflammation in Nrf2$^{-/-}$ mice, we analyzed the expression of cytokine genes (IL-6 and MCP-1) and inflammatory cell recruitment in the lungs of Nrf2$^{+/+}$, Nrf2$^{-/-}$, and Nrf2$^{-/-}$//gp91$^{phox-/-}$ mice after LPS treatment. Previously, we found that i.p. administration of LPS caused greater expression of IL-6, MCP-1, and other cytokines as early as 1 h and remained high for 6 h in the lungs of Nrf2$^{-/-}$ mice compared with Nrf2$^{+/+}$ mice (17). To determine whether NADPH oxidase activity is responsible for the early cytokine expression in the lungs of Nrf2$^{-/-}$ mice, we measured cytokine expression in the lungs at 1 h and 6 h after LPS injection. There was nearly a 2-fold increase in the expression

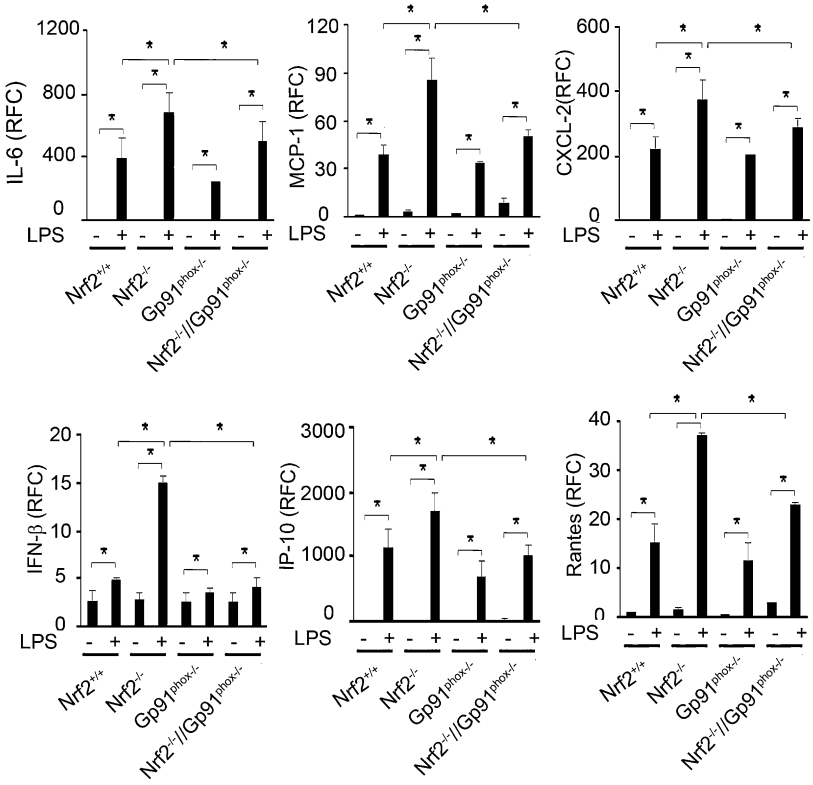

FIGURE 5. Genetic disruption of gp91^{phox} in Nrf2$^{-/-}$ macrophages alleviates LPS-induced expression of cytokines. mRNA expression of cytokines (IL-6, IFN-β, IP-10, and RANTES), and chemokines (MCP-1 and MIP-2) were evaluated in macrophages from Nrf2$^{+/+}$, Nrf2$^{-/-}$, gp91$^{phox-/-}$, and Nrf2$^{-/-}$// gp91$^{phox-/-}$ mice 4 h after LPS stimulation by QRT-PCR as described in *Materials and Methods*. Data are represented as mean ± SD, RCF from three independent experiments. $*p < 0.05$. RCF, relative fold change.

of IL-6 and MCP-1 in the lungs of Nrf2$^{-/-}$ compared with the lungs of Nrf2$^{+/+}$ mice after treatment with LPS (Fig. 6*A*; data shown only for 1-h treatment). However, disruption of NADPH oxidase in Nrf2$^{-/-}$ mice significantly reduced LPS-induced cytokine expression, and it was comparable to that in LPS-treated Nrf2$^{+/+}$ mice.

Next, we investigated whether disruption of gp91^{phox} in Nrf2$^{-/-}$ mice reduce pulmonary inflammation after LPS instillation. BAL fluid analysis showed greater recruitment of inflammatory cells (predominantly neutrophils [data not shown]) and IL-6 levels in Nrf2$^{-/-}$ mice compared with Nrf2$^{+/+}$ mice 6 h after LPS instillation (Fig. 6*B*, 6*C*). However, in Nrf2$^{-/-}$ mice treated with LPS, disruption of NADPH oxidase significantly reduced pulmonary inflammation, and this reduction was comparable to that in LPS-treated Nrf2$^{+/+}$ mice. No significant difference was detected in total cells and IL-6 levels between the genotypes treated with vehicle (data not shown). These results indicate that excess NADPH oxidase-dependent ROS was largely responsible for enhanced lung inflammation in Nrf2$^{-/-}$ mice.

Genetic disruption of gp91^{phox} in Nrf2$^{-/-}$ mice alleviates systemic inflammation and mortality after LPS shock or polymicrobial sepsis

Mortality in mice after LPS shock or polymicrobial sepsis is mediated by hyperactive inflammatory responses (38). We have shown that LPS shock and or polymicrobial sepsis caused greater mortality in Nrf2$^{-/-}$ mice compared with Nrf2$^{+/+}$ mice (9). To determine whether excess NADPH oxidase-dependent ROS generation mediates mortality in Nrf2$^{-/-}$ mice, we subjected Nrf2$^{+/+}$, Nrf2$^{-/-}$, and Nrf2$^{-/-}$//gp91$^{phox-/-}$ mice to CLP-induced sepsis or LPS shock. Mortality in Nrf2$^{+/+}$ mice was 20%, compared with 100% in Nrf2$^{-/-}$ mice 60 h after CLP shock. On the contrary, Nrf2$^{-/-}$//gp91$^{phox-/-}$ mice showed prolonged survival compared with Nrf2$^{-/-}$ mice after CLP shock. Mortality in Nrf2$^{-/-}$// gp91$^{phox-/-}$ mice was 40% and 80% at 60 h and 120 h, respectively, after CLP shock (Fig. 7*A*). All sham-treated mice survived (data not shown). Similarly, mortality was accelerated in Nrf2$^{-/-}$ mice after LPS shock compared with Nrf2$^{+/+}$ (Fig. 7*B*). However, disruption of gp91^{phox} in Nrf2$^{-/-}$ mice significantly prolonged the survival. Consistent with the results from previous studies, the mortality in gp91$^{phox-/-}$ mice was similar to Nrf2$^{+/+}$ mice [data not shown (41)]. As a marker of systemic inflammation, we measured serum IL-6 levels in Nrf2$^{+/+}$, Nrf2$^{-/-}$, and Nrf2$^{-/-}$// gp91$^{phox-/-}$ mice. After CLP and LPS shock, IL-6 was higher in the serum of Nrf2$^{-/-}$ mice; whereas, it was similar in Nrf2$^{+/+}$ and Nrf2$^{-/-}$//gp91$^{phox-/-}$ mice (Fig. 7*C*, 7*D*). Taken together, these data suggest that enhanced inflammatory response due to NADPH oxidase-dependent ROS signaling leads to increased mortality in Nrf2$^{-/-}$ mice after LPS and/or polymicrobial sepsis.

Discussion

ROS generated by NADPH oxidase plays a central role in the pathobiology of sepsis. NADPH oxidase-dependent ROS generation is important for the bactericidal activity by phagocytes, redox regulation of cellular signaling, and other physiological processes (42, 43). However, excessive levels of ROS may induce hyperactivation of innate immune cells (macrophages and neutrophils) (5, 6, 44), cytokine expression, vascular endothelial dysfunction, and end-organ injury (42, 43, 45–48). Therefore, the pathways that regulate ROS homeostasis are crucial for mediating a heightened but controlled immune inflammatory response.

The mortality in patients with sepsis as well as in an experimental model of sepsis is well correlated with inappropriate activation of the innate immune response (38). The ROS-mediated signaling events in modulating innate immune activation and mortality during sepsis are poorly understood. Nrf2 is a primary regulator of cellular antioxidants in response to diverse stimuli, including LPS (13, 49). Previously, we reported that polymicrobial sepsis- and LPS-induced shock caused greater mortality in Nrf2$^{-/-}$ mice compared with Nrf2$^{+/+}$ mice (17) that was partly due to a hyperactive innate immune response, which resulted in an early cytokine response. The temporal global gene expression

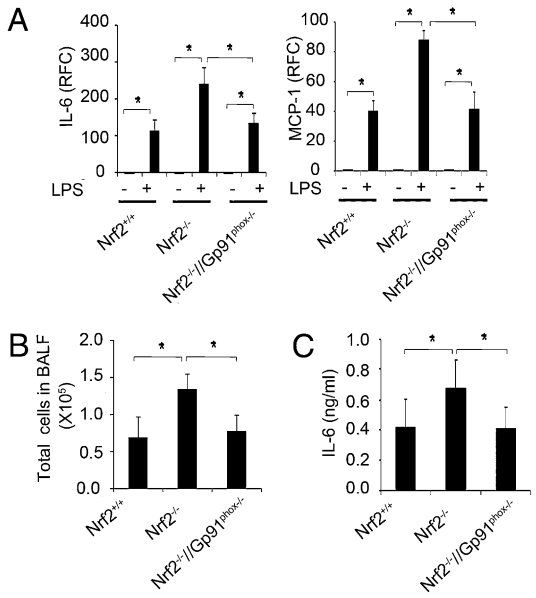

FIGURE 6. Genetic disruption of gp91^{phox} in Nrf2$^{-/-}$ mice attenuates LPS-induced pulmonary inflammation. *A*, mRNA expression of cytokines (IL-6), and chemokines (MCP-1) in the lungs of Nrf2$^{+/+}$, Nrf2$^{-/-}$, and Nrf2$^{-/-}$//gp91$^{phox-/-}$ mice 1 h after LPS administration (15 mg/kg body weight; i.p.). Data are represented as mean ± SD of RFC; n = 4 mice/group. *B*, Total cells in the BAL fluid from Nrf2$^{+/+}$, Nrf2$^{-/-}$, and Nrf2$^{-/-}$//gp91$^{phox-/-}$ mice 6 h after LPS administration. No significant difference was detected between the genotypes after vehicle treatment (data not shown). Data are represented as mean ± SD of total number of cells in BAL from 5 mice/group. *C*, IL-6 levels in the BAL fluid collected in *B*. IL-6 levels were measured by ELISA, n = 5 mice/group. IL-6 levels were below the detection limit in the BAL fluid of vehicle-treated mice group (data not shown). $*p < 0.05$. RFC, relative fold change.

analysis revealed higher expression of several cytokines and chemokines at early time points (<6 h) in the lungs of Nrf2$^{-/-}$ mice compared with Nrf2$^{+/+}$ mice after LPS treatment (17). However, the expression of these cytokines was similar in the lungs of Nrf2$^{+/+}$ and Nrf2$^{-/-}$ mice at 12 h and 24 h (17). In this study, we show that the early hyperactive innate immune response in Nrf2$^{-/-}$ mice was largely mediated by elevated NADPH oxidase activity. Disruption of gp91^{phox} in Nrf2$^{-/-}$ mice significantly reduced LPS-induced systemic and lung inflammation and this reduction was comparable to that in LPS-treated Nrf2$^{+/+}$ mice. Furthermore, disruption of gp91^{phox} significantly prolonged the survival of Nrf2$^{-/-}$ mice after LPS shock and CLP and the survival was comparable to that in LPS-treated Nrf2$^{+/+}$ mice. These data suggest that similar to ROS producers, cellular antioxidants are crucial modifiers of sepsis pathogenesis. Intriguingly, recent studies have found that NADPH oxidase-mediated ROS generation may be required for the activation of the Nrf2 signaling pathway (50, 51). We speculate that in Nrf2$^{-/-}$ mice, abrogation of Nrf2-regulated antioxidants enhances pathological effect of NADPH oxidase-induced ROS generation.

There are several sources of ROS in leukocytes including mitochondria, xanthine oxidase, and NADPH oxidases. ROS production after LPS stimulation in leukocytes is primarily mediated by NADPH oxidase activation (42). Previously, we reported that compared with Nrf2$^{+/+}$, LPS stimulation induced greater ROS generation in macrophages and neutrophils from Nrf2$^{-/-}$ mice that was abolished by diphenyleneiodonium, a nonspecific pharmacological inhibitor of NADPH oxidase (24). In the current study, it is evident that NADPH oxidase is the primary producer of ROS in macrophages of Nrf2$^{-/-}$ mice. LPS-induced levels of ROS in macrophages from Nrf2$^{-/-}$ mice was significantly reduced by ablation of gp91^{phox}, and it was comparable to that in the LPS-treated Nrf2$^{+/+}$ macrophages. Because Nrf2 disruption impaired induction of antioxidants, we assumed that higher levels of ROS in Nrf2$^{-/-}$ macrophages in response to LPS were due to decreased capacity to detoxify the ROS. However, in response to LPS, we observed greater activation of NADPH oxidase as indicated by higher phosphorylation of p47^{phox} in Nrf2$^{-/-}$ macrophages compared with Nrf2$^{+/+}$ macrophages. Phosphorylation of p47^{phox} is a key event for its translocation from the cytosol to the membrane, where it associates with a heterodimer of p22^{phox} and gp91^{phox} and other membrane integrated proteins to form a functional oxidase complex (9). LPS-induced phosphorylation of p47^{phox} in macrophages is mediated by PKC activity (31). We found higher PKC activity in Nrf2$^{-/-}$ macrophages compared

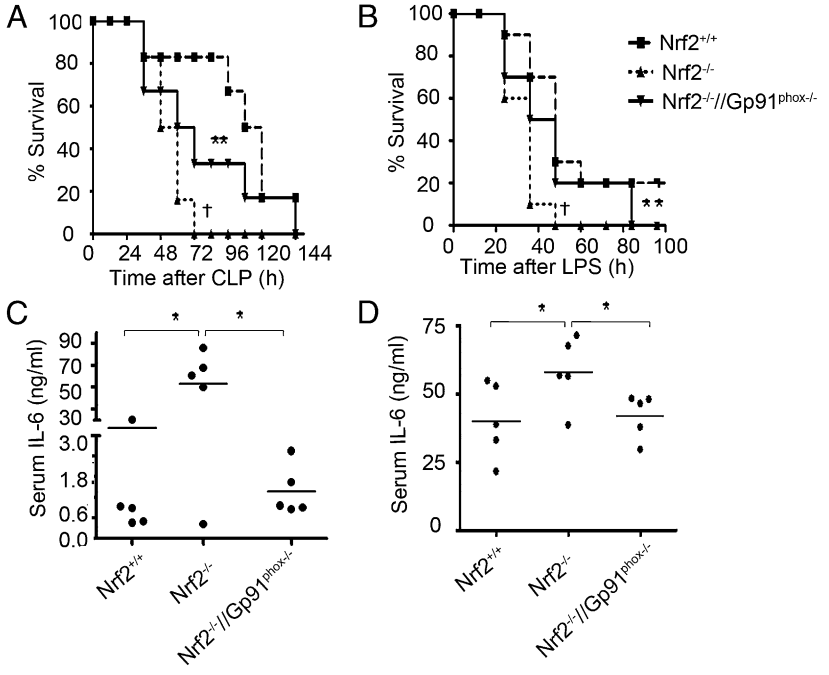

FIGURE 7. Genetic disruption of gp91^{phox} in Nrf2$^{-/-}$ mice alleviates systemic inflammation and improves survival after polymicrobial sepsis and LPS shock. *A*, A graph of the Kaplan-Meier survival curves of Nrf2$^{+/+}$, Nrf2$^{-/-}$, and Nrf2$^{-/-}$//gp91$^{phox-/-}$ mice after CLP (n = 10/gp); sham surgery caused no death (data not shown). After CLP procedure as described in *Materials and Methods*, mice were monitored every 12 h for 7 d. *B*, A graph of the Kaplan-Meier survival curves of mice (Nrf2$^{+/+}$, Nrf2$^{-/-}$, and Nrf2$^{-/-}$//gp91$^{phox-/-}$) after lethal dose of LPS administration (35 mg/kg bodyweight, i.p, (n = 10/gp); data were analyzed using log-rank test. †Significant compared with Nrf2$^{-/-}$, $p < 0.05$; **significant compared with Nrf2$^{-/-}$, $p < 0.01$. *C*, IL-6 levels in the serum 24 h after CLP, n = 5 mice/group. *D*, IL-6 levels in the serum 6 h after LPS administration. IL-6 levels were measured by ELISA, n = 5 mice/group. Serum IL-6 levels were below the detection limit in sham and/or vehicle-treated mice group (data not shown). $*p <$ 0.05.

with $Nrf2^{+/+}$ macrophages after LPS stimulation. GSH inhibits PKC activity via nonredox mechanisms (32, 33). In agreement, we found higher levels of GSH in $Nrf2^{+/+}$ macrophages compared with $Nrf2^{-/-}$ macrophages, and we also showed that depletion of GSH by BSO elevated PKC activity only in $Nrf2^{+/+}$ macrophages but not in $Nrf2^{-/-}$ macrophages after LPS stimulation. Furthermore, we also observed significant inhibition of LPS-induced ROS levels after PKC inhibition in $Nrf2^{-/-}$ macrophages. Taken together, these results suggest that there was a higher generation of NADPH oxidase-dependent ROS after LPS stimulation in $Nrf2^{-/-}$ macrophages.

It is well recognized that ROS modulate TLR4 signal transduction at multiple levels and subsequently activate NF-κB and IRF3. Pretreatment of neutrophils by the exogenous antioxidant N-acetylcysteine dampened LPS-induced TLR4 downstream signaling events, including activation of IL-1R–associated kinase-1 and -4, MAP kinases (ERK1/2, Akt, and p38), and IKKB (44). Previously, we have shown that LPS led to greater induction of IKK kinase activity, phosphorylation of IκB, and activation of NF-κB in $Nrf2^{-/-}$ macrophages compared with $Nrf2^{+/+}$ macrophages (17). However, the upstream signaling events that caused the activation of IKK kinase in $Nrf2^{-/-}$ macrophages are not known. A growing body of evidence indicates that the NADPH oxidase family modulates TLR4 signaling either by direct or indirect interactions via ROS generation (11, 52). ROS has been shown to enhance TLR4 translocation from the cytosol to lipid rafts in response to LPS stimulation that was inhibited by ablation of NADPH oxidase activity (39, 40). H_2O_2 treatment also enhanced TLR4 trafficking to lipid rafts in macrophages, indicating oxidant signaling in TLR4 activation (40). Because $Nrf2^{-/-}$ macrophages are associated with higher NADPH-induced ROS after LPS stimulation, we investigated whether this affects TLR4 activation. We found that LPS stimulation caused ~2-fold increase in the surface expression of TLR4 in macrophages and neutrophils isolated from $Nrf2^{-/-}$ mice, compared with $Nrf2^{+/+}$ mice. However, disruption of NADPH oxidase significantly suppressed TLR4 surface expression in $Nrf2^{-/-}$ macrophages to a level similar to that seen in $Nrf2^{+/+}$ macrophages. On ligand binding, adapter molecules MyD88 and TRIF interact with the cytoplasmic domain of TLR4 (53). We observed that in LPS-treated $Nrf2^{-/-}$ macrophages, there was a greater recruitment of adapter proteins MyD88 and TRIF to TLR4. In line with these results, we noted higher levels of phosphorylation of IκB and IRF3 and cytokine expression (IL-6, MCP-1, MIP-2, and RANTES) in LPS-treated $Nrf2^{-/-}$ macrophages. In contrast, disruption of $gp91^{phox}$ in LPS-treated $Nrf2^{-/-}$ macrophages markedly reduced the TLR4 downstream signaling events from complex formation with adapter molecules to cytokine expression. These events were comparable to that in the LPS-treated $Nrf2^{+/+}$ macrophages. Overall, we elucidated the role of Nrf2-dependent cellular antioxidants in redox regulation of TLR4 signaling, an early critical event in the pathogenesis of sepsis.

In a recent study, it is demonstrated that coordinated action of multiple Nrf2-regulated antioxidants (Nqo1 and heme oxygenase 1) results in robust protection against LPS-induced inflammatory responses (49), unlike the action of a single antioxidant protein. Therefore, regulation of Nrf2-dependent cellular antioxidants is critical to limit ROS-mediated dysregulation of the innate immune response in sepsis.

Disclosures

The authors have no financial conflicts of interest.

References

1. Riedemann, N. C., R. F. Guo, and P. A. Ward. 2003. Novel strategies for the treatment of sepsis. *Nat. Med.* 9: 517–524.
2. Akira, S. 2006. TLR signaling. *Curr. Top. Microbiol. Immunol.* 311: 1–16.
3. Akira, S., and K. Takeda. 2004. Toll-like receptor signalling. *Nat. Rev. Immunol.* 4: 499–511.
4. Fink, M. P. 2002. Reactive oxygen species as mediators of organ dysfunction caused by sepsis, acute respiratory distress syndrome, or hemorrhagic shock: potential benefits of resuscitation with Ringer's ethyl pyruvate solution. *Curr. Opin. Clin. Nutr. Metab. Care* 5: 167–174.
5. Lorne, E., J. W. Zmijewski, X. Zhao, G. Liu, Y. Tsuruta, Y. J. Park, H. Dupont, and E. Abraham. 2008. Role of extracellular superoxide in neutrophil activation: interactions between xanthine oxidase and TLR4 induce proinflammatory cytokine production. *Am. J. Physiol. Cell Physiol.* 294: C985–C993.
6. Mitra, S., and E. Abraham. 2006. Participation of superoxide in neutrophil activation and cytokine production. *Biochim. Biophys. Acta* 1762: 732–741.
7. Fan, J., R. S. Frey, and A. B. Malik. 2003. TLR4 signaling induces TLR2 expression in endothelial cells via neutrophil NADPH oxidase. *J. Clin. Invest.* 112: 1234–1243.
8. Kolls, J. K. 2006. Oxidative stress in sepsis: a redox redux. *J. Clin. Invest.* 116: 860–863.
9. Lambeth, J. D. 2004. NOX enzymes and the biology of reactive oxygen. *Nat. Rev. Immunol.* 4: 181–189.
10. Dröge, W. 2002. Free radicals in the physiological control of cell function. *Physiol. Rev.* 82: 47–95.
11. Park, H. S., H. Y. Jung, E. Y. Park, J. Kim, W. J. Lee, and Y. S. Bae. 2004. Cutting edge: direct interaction of TLR4 with NAD(P)H oxidase 4 isozyme is essential for lipopolysaccharide-induced production of reactive oxygen species and activation of NF-kappa B. *J. Immunol.* 173: 3589–3593.
12. Imai, Y., K. Kuba, G. G. Neely, R. Yaghubian-Malhami, T. Perkmann, G. van Loo, M. Ermolaeva, R. Veldhuizen, Y. H. Leung, H. Wang, et al. 2008. Identification of oxidative stress and Toll-like receptor 4 signaling as a key pathway of acute lung injury. *Cell* 133: 235–249.
13. Kensler, T. W., N. Wakabayashi, and S. Biswal. 2007. Cell survival responses to environmental stresses via the Keap1-Nrf2-ARE pathway. *Annu. Rev. Pharmacol. Toxicol.* 47: 89–116.
14. Cho, H. Y., S. P. Reddy, M. Yamamoto, and S. R. Kleeberger. 2004. The transcription factor NRF2 protects against pulmonary fibrosis. *FASEB J.* 18: 1258–1260.
15. Rangasamy, T., C. Y. Cho, R. K. Thimmulappa, L. Zhen, S. S. Srisuma, T. W. Kensler, M. Yamamoto, I. Petrache, R. M. Tuder, and S. Biswal. 2004. Genetic ablation of Nrf2 enhances susceptibility to cigarette smoke-induced emphysema in mice. *J. Clin. Invest.* 114: 1248–1259.
16. Rangasamy, T., J. Guo, W. A. Mitzner, J. Roman, A. Singh, A. D. Fryer, M. Yamamoto, T. W. Kensler, R. M. Tuder, S. N. Georas, and S. Biswal. 2005. Disruption of Nrf2 enhances susceptibility to severe airway inflammation and asthma in mice. *J. Exp. Med.* 202: 47–59.
17. Thimmulappa, R. K., H. Lee, T. Rangasamy, S. P. Reddy, M. Yamamoto, T. W. Kensler, and S. Biswal. 2006. Nrf2 is a critical regulator of the innate immune response and survival during experimental sepsis. *J. Clin. Invest.* 116: 984–995.
18. Wang, J., J. Fields, C. Zhao, J. Langer, R. K. Thimmulappa, T. W. Kensler, M. Yamamoto, S. Biswal, and S. Doré. 2007. Role of Nrf2 in protection against intracerebral hemorrhage injury in mice. *Free Radic. Biol. Med.* 43: 408–414.
19. Khor, T. O., M. T. Huang, K. H. Kwon, J. Y. Chan, B. S. Reddy, and A. N. Kong. 2006. Nrf2-deficient mice have an increased susceptibility to dextran sulfate sodium-induced colitis. *Cancer Res.* 66: 11580–11584.
20. Osburn, W. O., B. Karim, P. M. Dolan, G. Liu, M. Yamamoto, D. L. Huso, and T. W. Kensler. 2007. Increased colonic inflammatory injury and formation of aberrant crypt foci in Nrf2-deficient mice upon dextran sulfate treatment. *Int. J. Cancer* 121: 1883–1891.
21. Malhotra, D., R. Thimmulappa, A. Navas-Acien, A. Sandford, M. Elliott, A. Singh, L. Chen, X. Zhuang, J. Hogg, P. Pare, et al. 2008. Decline in NRF2-regulated antioxidants in chronic obstructive pulmonary disease lungs due to loss of its positive regulator, DJ-1. *Am. J. Respir. Crit. Care Med.* 178: 592–604.
22. Nagai, N., R. K. Thimmulappa, M. Cano, M. Fujihara, K. Izumi-Nagai, X. Kong, M. B. Sporn, T. W. Kensler, S. Biswal, and J. T. Handa. 2009. Nrf2 is a critical modulator of the innate immune response in a model of uveitis. *Free Radic. Biol. Med.* 47: 300–306.
23. Innamorato, N. G., A. I. Rojo, A. J. García-Yagüe, M. Yamamoto, M. L. de Ceballos, and A. Cuadrado. 2008. The transcription factor Nrf2 is a therapeutic target against brain inflammation. *J. Immunol.* 181: 680–689.
24. Thimmulappa, R. K., C. Scollick, K. Traore, M. Yates, M. A. Trush, K. T. Liby, M. B. Sporn, M. Yamamoto, T. W. Kensler, and S. Biswal. 2006. Nrf2-dependent protection from LPS induced inflammatory response and mortality by CDDO-Imidazolide. *Biochem. Biophys. Res. Commun.* 351: 883–889.
25. Sussan, T. E., T. Rangasamy, D. J. Blake, D. Malhotra, and H. El. Haddad, D. Bedja, M. S. Yates, P. Kombairaju, M. Yamamoto, K. T. Liby, M. B. Sporn, K. L. Gabrielson, H. C. Champion, R. M. Tuder, T. W. Kensler, and S. Biswal. 2009. Targeting Nrf2 with the triterpenoid CDDO-imidazolide attenuates cigarette smoke-induced emphysema and cardiac dysfunction in mice. *Proc Natl Acad Sci U S A* 106:250-255.
26. Singh, A., S. Boldin-Adamsky, R. K. Thimmulappa, S. K. Rath, H. Ashush, J. Coulter, A. Blackford, S. N. Goodman, F. Bunz, W. H. Watson, et al. 2008. RNAi-mediated silencing of nuclear factor erythroid-2-related factor 2 gene expression in non-small cell lung cancer inhibits tumor growth and increases efficacy of chemotherapy. *Cancer Res.* 68: 7975–7984.
27. Mukhopadhyay, P., M. Rajesh, G. Haskó, B. J. Hawkins, M. Madesh, and P. Pacher. 2007. Simultaneous detection of apoptosis and mitochondrial

superoxide production in live cells by flow cytometry and confocal microscopy. *Nat. Protoc.* 2: 2295–2301.
28. Trachootham, D., J. Alexandre, and P. Huang. 2009. Targeting cancer cells by ROS-mediated mechanisms: a radical therapeutic approach? *Nat. Rev. Drug Discov.* 8: 579–591.
29. Griffith, O. W., and A. Meister. 1979. Potent and specific inhibition of glutathione synthesis by buthionine sulfoximine (S-n-butyl homocysteine sulfoximine). *J. Biol. Chem.* 254: 7558–7560.
30. Fontayne, A., P. M. Dang, M. A. Gougerot-Pocidalo, and J. El-Benna. 2002. Phosphorylation of p47phox sites by PKC alpha, beta II, delta, and zeta: effect on binding to p22phox and on NADPH oxidase activation. *Biochemistry* 41: 7743–7750.
31. Bey, E. A., B. Xu, A. Bhattacharjee, C. M. Oldfield, X. Zhao, Q. Li, V. Subbulakshmi, G. M. Feldman, F. B. Wientjes, and M. K. Cathcart. 2004. Protein kinase C delta is required for p47phox phosphorylation and translocation in activated human monocytes. *J. Immunol.* 173: 5730–5738.
32. Ward, N. E., D. S. Pierce, S. E. Chung, K. R. Gravitt, and C. A. O'Brian. 1998. Irreversible inactivation of protein kinase C by glutathione. *J. Biol. Chem.* 273: 12558–12566.
33. Domenicotti, C., B. Marengo, D. Verzola, G. Garibotto, N. Traverso, S. Patriarca, G. Maloberti, D. Cottalasso, G. Poli, M. Passalacqua, et al. 2003. Role of PKC-delta activity in glutathione-depleted neuroblastoma cells. *Free Radic. Biol. Med.* 35: 504–516.
34. Combadière, C., E. Pedruzzi, J. Hakim, and A. Périanin. 1993. A protein kinase inhibitor, staurosporine, enhances the expression of phorbol dibutyrate binding sites in human polymorphonuclear leucocytes. *Biochem. J.* 289: 695–701.
35. Wang, D., D. Malo, and S. Hekimi. 2010. Elevated mitochondrial reactive oxygen species generation affects the immune response via hypoxia-inducible factor-1alpha in long-lived Mclk1+/- mouse mutants. *J. Immunol.* 184: 582–590.
36. Zmijewski, J. W., E. Lorne, X. Zhao, Y. Tsuruta, Y. Sha, G. Liu, G. P. Siegal, and E. Abraham. 2008. Mitochondrial respiratory complex I regulates neutrophil activation and severity of lung injury. *Am. J. Respir. Crit. Care Med.* 178: 168–179.
37. Roger, T., C. Froidevaux, D. Le Roy, M. K. Reymond, A. L. Chanson, D. Mauri, K. Burns, B. M. Riederer, S. Akira, and T. Calandra. 2009. Protection from lethal gram-negative bacterial sepsis by targeting Toll-like receptor 4. *Proc. Natl. Acad. Sci. USA* 106: 2348–2352.
38. Rittirsch, D., M. A. Flierl, and P. A. Ward. 2008. Harmful molecular mechanisms in sepsis. *Nat. Rev. Immunol.* 8: 776–787.
39. Nakahira, K., H. P. Kim, X. H. Geng, A. Nakao, X. Wang, N. Murase, P. F. Drain, X. Wang, M. Sasidhar, E. G. Nabel, et al. 2006. Carbon monoxide differentially inhibits TLR signaling pathways by regulating ROS-induced trafficking of TLRs to lipid rafts. *J. Exp. Med.* 203: 2377–2389.
40. Powers, K. A., K. Szászi, R. G. Khadaroo, P. S. Tawadros, J. C. Marshall, A. Kapus, and O. D. Rotstein. 2006. Oxidative stress generated by hemorrhagic shock recruits Toll-like receptor 4 to the plasma membrane in macrophages. *J. Exp. Med.* 203: 1951–1961.
41. Zhang, W. J., H. Wei, and B. Frei. 2009. Genetic deficiency of NADPH oxidase does not diminish, but rather enhances, LPS-induced acute inflammatory responses in vivo. *Free Radic. Biol. Med.* 46: 791–798.
42. Bedard, K., and K. H. Krause. 2007. The NOX family of ROS-generating NADPH oxidases: physiology and pathophysiology. *Physiol. Rev.* 87: 245–313.
43. Krause, K. H., and K. Bedard. 2008. NOX enzymes in immuno-inflammatory pathologies. *Semin. Immunopathol.* 30: 193–194.
44. Asehnoune, K., D. Strassheim, S. Mitra, J. Y. Kim, and E. Abraham. 2004. Involvement of reactive oxygen species in Toll-like receptor 4-dependent activation of NF-kappa B. *J. Immunol.* 172: 2522–2529.
45. Tyml, K., F. Li, and J. X. Wilson. 2008. Septic impairment of capillary blood flow requires nicotinamide adenine dinucleotide phosphate oxidase but not nitric oxide synthase and is rapidly reversed by ascorbate through an endothelial nitric oxide synthase-dependent mechanism. *Crit. Care Med.* 36: 2355–2362.
46. Wang, W., Y. Suzuki, T. Tanigaki, D. R. Rank, and T. A. Raffin. 1994. Effect of the NADPH oxidase inhibitor apocynin on septic lung injury in guinea pigs. *Am. J. Respir. Crit. Care Med.* 150: 1449–1452.
47. Li, X., M. G. Schwacha, I. H. Chaudry, and M. A. Choudhry. 2008. Heme oxygenase-1 protects against neutrophil-mediated intestinal damage by down-regulation of neutrophil p47phox and p67phox activity and O2- production in a two-hit model of alcohol intoxication and burn injury. *J. Immunol.* 180: 6933–6940.
48. Wu, F., D. P. Schuster, K. Tyml, and J. X. Wilson. 2007. Ascorbate inhibits NADPH oxidase subunit p47phox expression in microvascular endothelial cells. *Free Radic. Biol. Med.* 42: 124–131.
49. Rushworth, S. A., D. J. MacEwan, and M. A. O'Connell. 2008. Lipopolysaccharide-induced expression of NAD(P)H:quinone oxidoreductase 1 and heme oxygenase-1 protects against excessive inflammatory responses in human monocytes. *J. Immunol.* 181: 6730–6737.
50. Lee, I. T., S. W. Wang, C. W. Lee, C. C. Chang, C. C. Lin, S. F. Luo, and C. M. Yang. 2008. Lipoteichoic acid induces HO-1 expression via the TLR2/MyD88/c-Src/NADPH oxidase pathway and Nrf2 in human tracheal smooth muscle cells. *J. Immunol.* 181: 5098–5110.
51. Sekhar, K. R., P. A. Crooks, V. N. Sonar, D. B. Friedman, J. Y. Chan, M. J. Meredith, J. H. Starnes, K. R. Kelton, S. R. Summar, S. Sasi, and M. L. Freeman. 2003. NADPH oxidase activity is essential for Keap1/Nrf2-mediated induction of GCLC in response to 2-indol-3-yl-methylenequinuclidin-3-ols. *Cancer Res.* 63: 5636–5645.
52. Singh, A., K. A. Zarember, D. B. Kuhns, and J. I. Gallin. 2009. Impaired priming and activation of the neutrophil NADPH oxidase in patients with IRAK4 or NEMO deficiency. *J. Immunol.* 182: 6410–6417.
53. Takeda, K., and S. Akira. 2004. TLR signaling pathways. *Semin. Immunol.* 16: 3–9.